CHEMPHYSCHEM

Supporting Information

Chemistries for Patterning Robust DNA MicroBarcodes Enable Multiplex Assays of Cytoplasm Proteins from Single Cancer Cells

Young Shik Shin,[a, b] Habib Ahmad,[a] Qihui Shi,[a] Hyungjun Kim,[c] Tod A. Pascal,[c] Rong Fan,[d] William A. Goddard III,[c] and James R. Heath*[a]

cphc_201000528_sm_miscellaneous_information.pdf
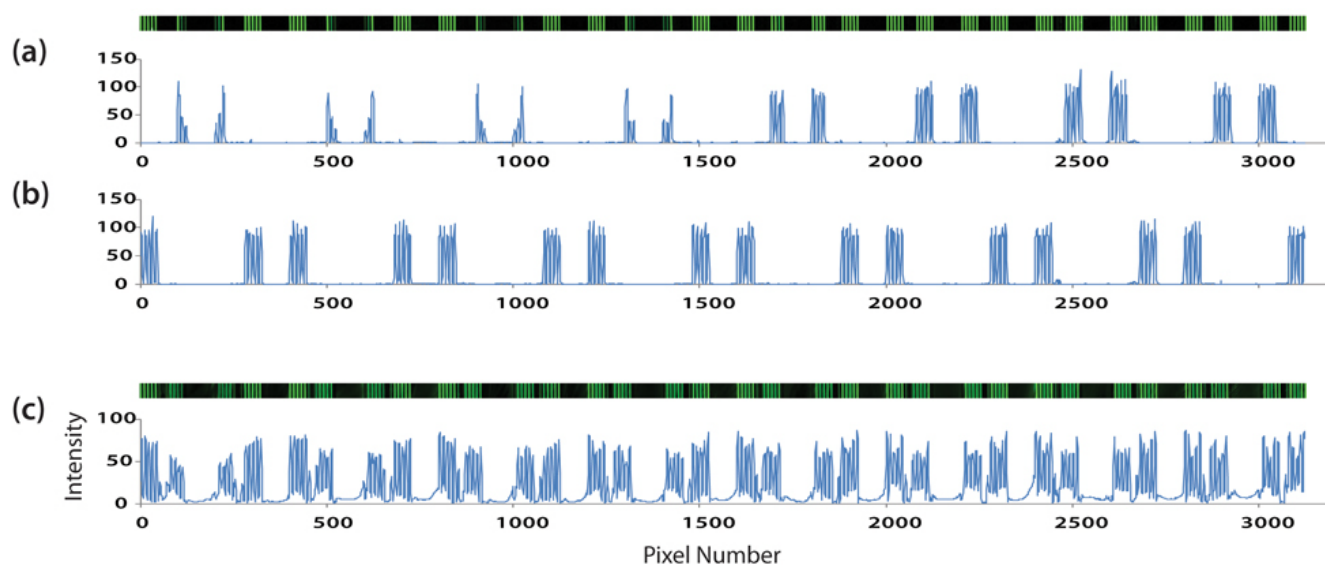
Supplementary Figures

Figure S1. Line profiles for the DNAs patterned by Scheme 1(a), Scheme 2 (b), and Scheme 3 (c). Y-axis is the intensity of the signal and x-axis is the pixel numbers. One pixel corresponds to 5 µm.
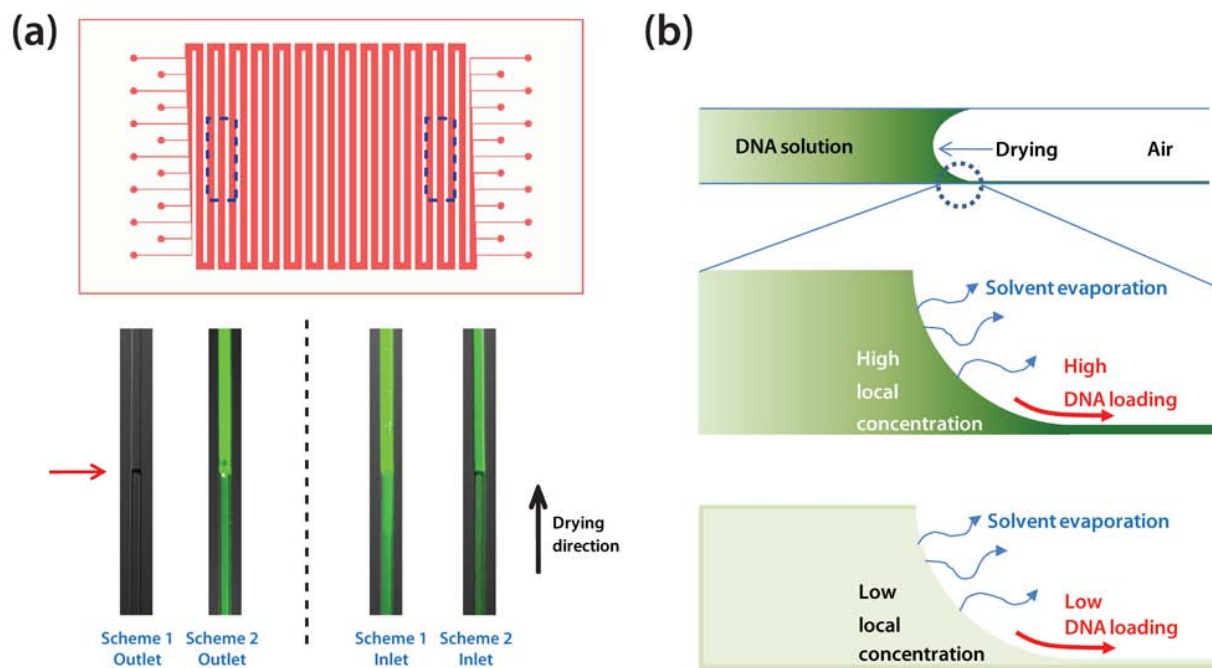

Figure S2. The microfluidic flow-patterning process to form the DNA barcodes. As the solvent evaporates through the PDMS elastomer, the concentration of the DNA oligomer solution increases. The oligomers are eventually deposited on the microchannel surfaces. **(a)** Fluorescence images of DNA solutions during the drying process for Schemes 1 and 2, in the region of the receding meniscus, and

near the outlet (left) and inlet (right) sides of the microchannel. Note that, at the inlet side, the fluorescence intensity near the receding meniscus is very high – evidence of the high local concentration of DNA due to solvent evaporation. The channel filled according to Scheme 1 exhibits no significant DNA near the channel outlet due to excessive electrostatically-driven depletion near the inlet side. The red arrow indicates the location of the meniscus. (b) Schematics for the drying process with different local concentrations. A high local concentration is required to achieve suitable DNA loading on the substrate.
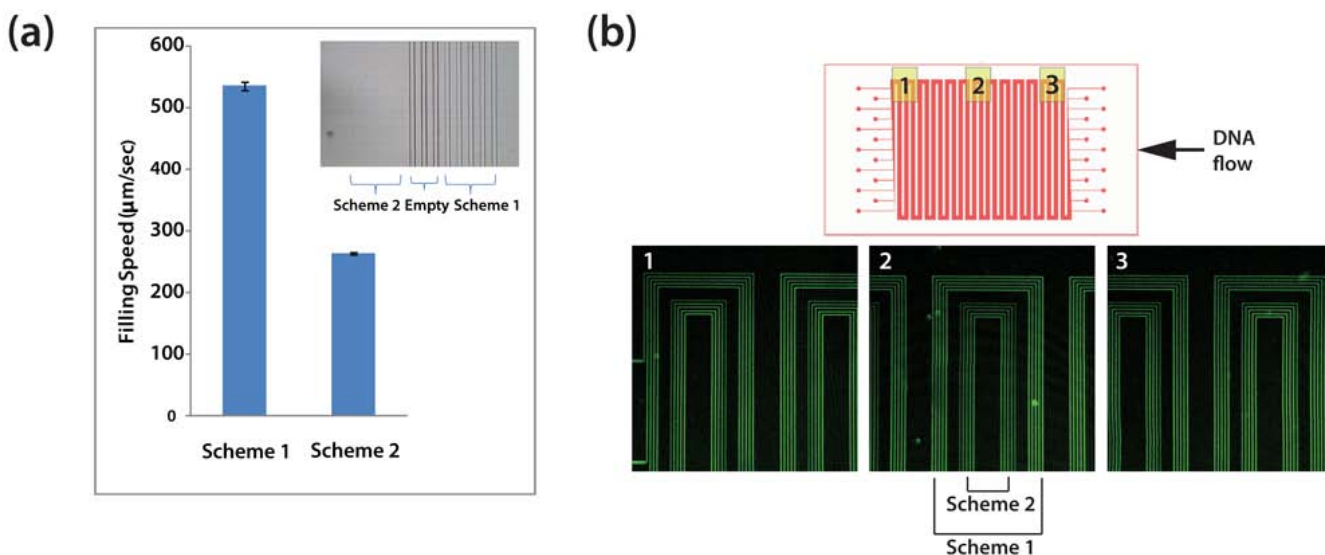

Figure S3. Results from experiments designed to more fully understand the effect of electrostatic adsorption of DNA within the microchannels during flow patterning. (a) Measurements of the flow speed of PBS solution of DNA oligomers (Scheme 1) and PBS/DMSO solution (Scheme 2) in the microfluidic channels. The filling process was optically monitored and recorded as a movie. The speed was calculated when the flow makes the fifth turn in the channel. The filling speed for Scheme 2 was less than that of Scheme 1, an observation that is attributable to the differential channel wetting between the two schemes (inset). The wetting of the PBS/DMSO Scheme 2 fluid was significantly better, a factor that minimizes bubble formation in the channel during the drying step. (b) Fluorescence images of DNA patterned within the microchannels of an O_2 plasma treated bare glass/PDMS device. The highly negative surface induced by plasma treatment minimizes electrostatic adsorption of DNA, resulting in uniform DNA distribution for both Scheme 1 and Scheme 2. The PDMS was solvent extracted just prior to bonding in order to prolong its hydrophilicity following plasma treatment.[1] Panels 1, 2, and 3 represent different locations in the flow patterning device.
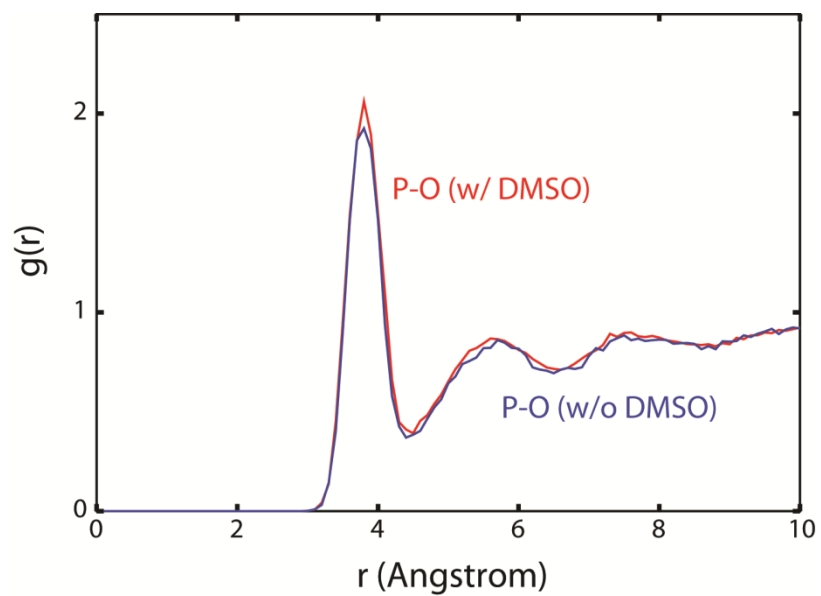
Figure S4. Molecular simulation result of the influence of DMSO in the Scheme 2 process. The radial distribution function of the P atom of the phosphate group of the DNA backbone and O atom of the water molecule is not influenced by the presence of DMSO.
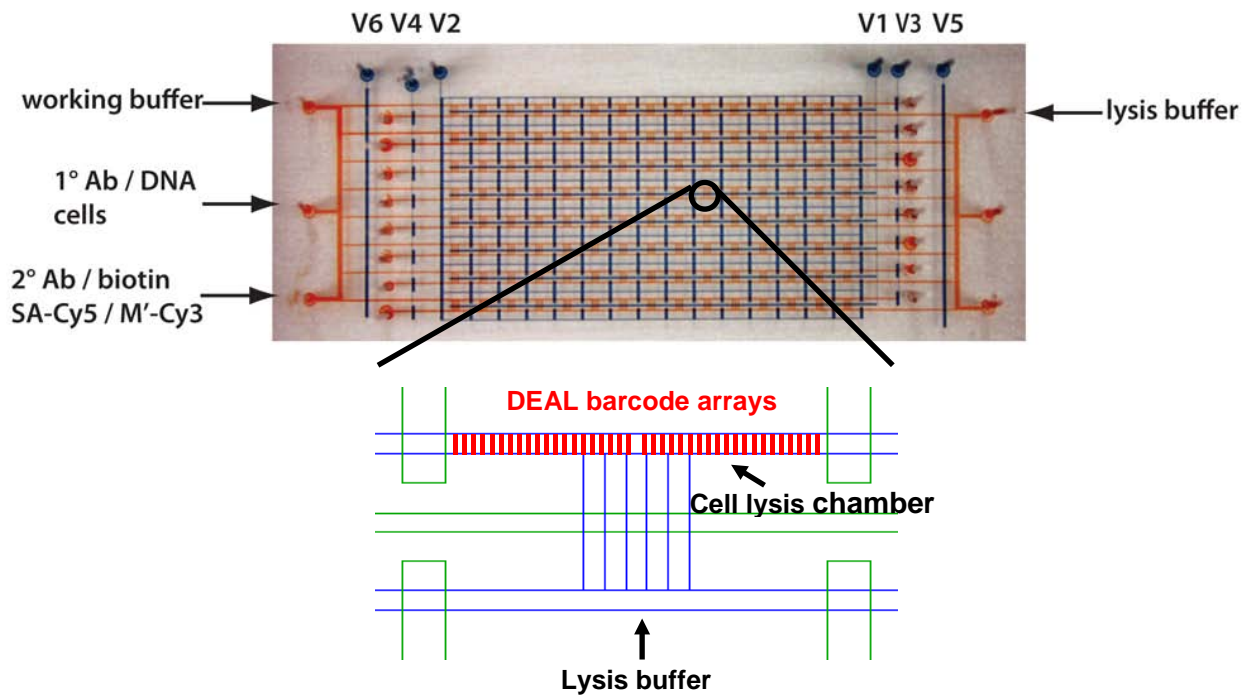
Figure S5. The Single Cell Barcode Chip (SCBC) utilized for on-chip cell lysis and multiplex intracellular protein detection. V1 to V6 represent valves. V1 is used to control the diffusion of the cell lysis buffer to the cell lysis chamber and closure of V2 results in the formation of isolated chambers from the long channels. V3, V4, V5, and V6 are utilized to control solution flows in the microchannels. Food dyes are used here to visualize the flow channels and control valves. The volume of each microchamber is ~2 nL.
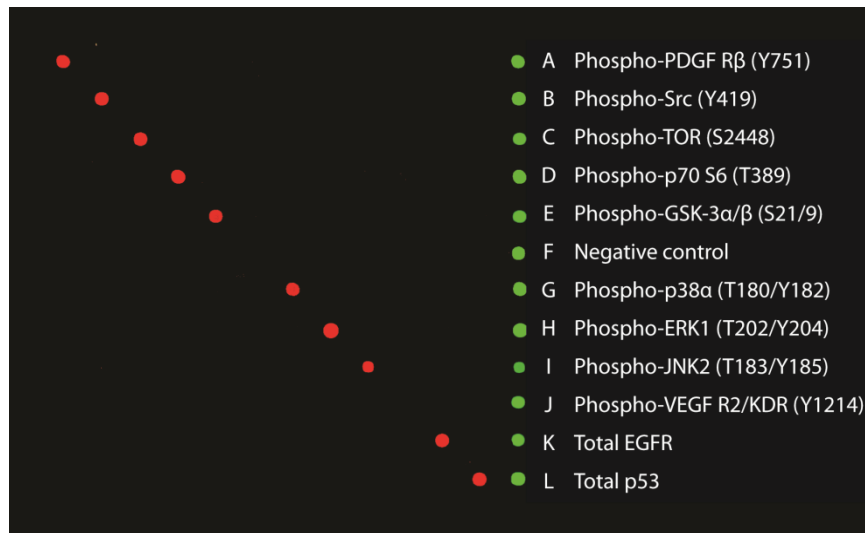
Figure S6. Antibody cross-reactivity tests. All antibodies were pre-selected based on such cross-reactivity tests. A pin-spotted DNA microarray was used for a DEAL-based protein detection approach - similar to the assays used within the SCBC microfluidic devices for single cell proteomics. Each row shows the results from different conditions. For all conditions, the same cocktail of DEAL conjugates was used, and included one conjugate for each of the 11 proteins assayed. For each row, only one target recombinant protein was tested. The target proteins were introduced at concentrations between 5-50 ng/mL, depending on the sensitivity of each antibody pair. Red spots are signals from the target proteins and the green spots are reference signals from Cy3-labeled DNA sequence M'. Phospho-VEGFR2 was not validated because the recombinant protein is not commercially available.
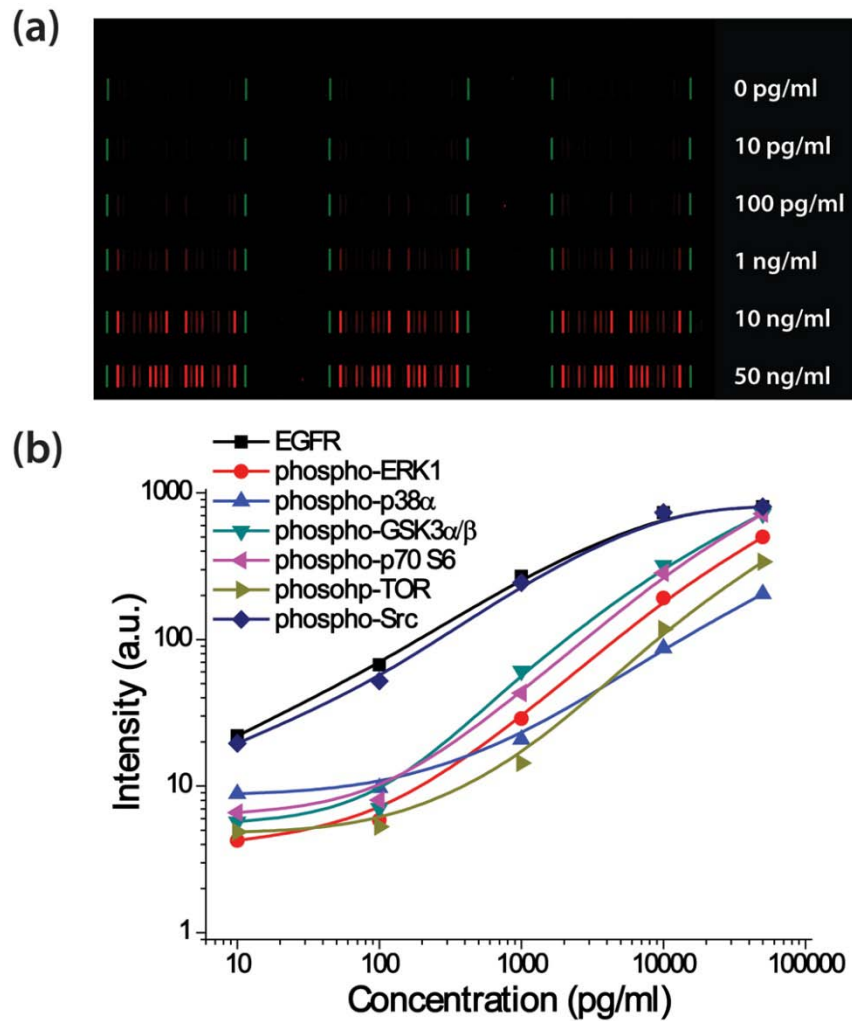
Figure S7. Calibration data for proteins in the panel. (a) Representative scanned images showing serial dilution measurements of selected proteins. Recombinant proteins were serially diluted (50 ng/mL, 10 ng/mL, 1 ng/mL, 100 pg/mL, 10 pg/mL and 0 pg/mL) in 1X PBS and flowed into the different microchannels of the microfluidic device for cell lysis analysis. Valves were immediately closed to compartmentalize standard proteins into microchambers followed by on-chip lysis buffer diffusion on ice for 2 hr. (b) Calibration curves of EGFR, p-ERK, p-p38α, p-GSK3α/β, p-p70S6K, p-mTOR and p-Src are plotted based on the results from a) to demonstrate the quantitative characteristics of the analysis. The sensitivities identified from the calibration curves are similar to standard ELISA sensitivities (e.g. EGFR: ~10 pg/mL, p-p70S6K: ~100 pg/mL, p-mTOR: ~200 pg/mL).

Supplementary Tables

Supplementary Table 1. Sequences and terminal functionalization of oligonucleotides: All oligonucleotides were synthesized by Integrated DNA Technology (IDT) and purified via high performance liquid chromatography (HPLC). The DNA coding oligomers were pre-tested for orthogonality to ensure that cross-hybridization between non-complementary oligomer strands was negligible (<1% in photon counts).

Name	Sequence	Melting Point
A	5'- AAA AAA AAA AAA AAT CCT GGA GCT AAG TCC GTA-3'	57.9
A'	5' NH3- AAA AAA AAA ATA CGG ACT TAG CTC CAG GAT-3'	57.2
B	5'-AAA AAA AAA AAA AGC CTC ATT GAA TCA TGC CTA -3'	57.4
B'	5' NH3AAA AAA AAA ATA GGC ATG ATT CAA TGA GGC -3'	55.9
C	5'- AAA AAA AAA AAA AGC ACT CGT CTA CTA TCG CTA -3'	57.6
C'	5' NH3-AAA AAA AAA ATA GCG ATA GTA GAC GAG TGC -3'	56.2
D	5'-AAA AAA AAA AAA AAT GGT CGA GAT GTC AGA GTA -3'	56.5
D'	5' NH3-AAA AAA AAA ATA CTC TGA CAT CTC GAC CAT -3'	55.7
E	5'-AAA AAA AAA AAA AAT GTG AAG TGG CAG TAT CTA -3'	55.7
E'	5' NH3-AAA AAA AAA ATA GAT ACT GCC ACT TCA CAT -3'	54.7
F	5'-AAA AAA AAA AAA AAT CAG GTA AGG TTC ACG GTA -3'	56.9
F'	5' NH3-AAA AAA AAA ATA CCG TGA ACC TTA CCT GAT -3'	56.1
G	5'-AAA AAA AAA AGA GTA GCC TTC CCG AGC ATT-3'	59.3
G'	5' NH3-AAA AAA AAA AAA TGC TCG GGA AGG CTA CTC-3'	58.6
H	5'-AAA AAA AAA AAT TGA CCA AAC TGC GGT GCG-3'	59.9
H'	5' NH3-AAA AAA AAA ACG CAC CGC AGT TTG GTC AAT-3'	60.8
I	5'-AAA AAA AAA ATG CCC TAT TGT TGC GTC GGA-3'	60.1
I'	5' NH3-AAA AAA AAA ATC CGA CGC AAC AAT AGG GCA-3'	60.1
J	5'-AAA AAA AAA ATC TTC TAG TTG TCG AGC AGG-3'	56.5
J'	5' NH3-AAA AAA AAA ACC TGC TCG ACA ACT AGA AGA-3'	57.5
K	5'-AAA AAA AAA ATA ATC TAA TTC TGG TCG CGG-3'	55.4
K'	5' NH3-AAA AAA AAA ACC GCG ACC AGA ATT AGA TTA-3'	56.3
L	5'-AAA AAA AAA AGT GAT TAA GTC TGC TTC GGC-3'	57.2
L'	5' NH3-AAA AAA AAA AGC CGA AGC AGA CTT AAT CAC-3'	57.2
M	5'-Cy3-AAA AAA AAA AGT CGA GGA TTC TGA ACC TGT-3'	57.6
M'	5' NH3-AAA AAA AAA AAC AGG TTC AGA ATC CTC GAC-3'	56.9

Supplementary Table 2. Summary of antibodies used for cell lysis experiments: All antibody pairs except p-VEGFR2 were purchased as ELISA kits of R&D systems (DuoSet® Elisa Development Reagents) containing capture antibodies, biotinylated detection antibodies and standard proteins. Capture antibodies bind both phosphoryalted and unphosphorylated proteins. The biotinylated detection antibodies detect only the phosphorylated variants of the proteins. VEGFR2 capture antibody, p-VEGFR2 (Y1214) detection antibodies were purchased from Abcam.

DNA label	Antibody	Source
A'	Human p-PDGFRβ (Y751) kit	R&D DYC3096
B'	Human p-Src (Y419) kit	R&D DYC2685
C'	Human p-mTOR (S2448) kit	R&D DYC1665
D'	Human p-p70S6K (T389) kit	R&D DYC896
E'	Human p-GSK3α/β (S21/S9) kit	R&D DYC2630
G'	Human p-p38α (T180/Y182) kit	R&D DYC869
H'	Human p-ERK (T202/Y204) kit	R&D DYC1825
I'	Human p-JNK2 (T183/Y185) kit	R&D DYC2236
K'	Human total EGFR kit	R&D DYC1854
L'	Human total P53 kit	R&D DYC1043
J'	Capture antibody: rabbit anti-human p-VEGFR2 (Y1214)	Abcam ab31480
	Detection antibody: biotin-labeled mouse anti-human VEGFR2	Abcam ab10975

Modeling of electrostatic adsorption of DNA to poly-L-lysine (PLL) surface

This modeling follows the approach used in reference 2. [2]
The following assumptions are used for the simulation:

- Nonspecific DNA adhesion to the PDMS surface is insignificant compared with the adhesion to the PLL surface
- DNAs are instantaneously and irreversibly captured to the PLL surface when they are transported to the surface

We start with the following mass transport equation,

$$v_x \frac{\partial C}{\partial x} = D \frac{\partial^2 C}{\partial y^2}$$

where v_x is the fluid velocity along the channel and y is the channel height. We can apply boundary conditions such that at the top and side walls, there are no concentration gradients.
In a rectangular channel, the mass diffusion coefficient, can be approximated by

$$h_{diff} = 3.81 \ D/d_h$$

where h_{diff} is the hydraulic channel diameter, $\frac{4 \ [cross-section \ area]}{[perimeter]}$.
As DNA flows down the channel during the initial filling step, DNA is electrostatically captured by PLL on the surface, causing a concentration gradient. Thus, the mean concentration of the sample at position x, C_x can be expressed as

$$C_x = C_i e^{-h_{diff} \ w \ x/Q}$$

where C_i is the sample concentration at the channel entrance.
We are interested in how C_x changes as the sample flows along the channel and we can simply apply the parameters of our system.
It has been reported that the diffusion coefficients of labeled single-strand DNA are predicted by:

$$D_{label} = 4 \times 10^{-6} B^{-0.539}$$

where B is the number of bases.[3-4]
In order to calculate C_x, we need the flow velocity. We measured the DNA sample filling speed (Fig. S3a) and used 536 μm/sec for simulation.

References

[1] J. A. Vickers, M. M. Caulum, C. S. Henry *Analytical Chemistry*. **2006**, 78, 7446-7452.
[2] J. A. Benn, J. Hu, B. J. Hogan, R. C. Fry, L. D. Samson, T. Thorsen *Anal Biochem*. **2006**, 348, 284-293.
[3] B. Tinland, A. Pluen, J. Sturm, G. Weill *Macromolecules*. **1997**, 30, 5763-5765.
[4] A. E. Nkodo, J. M. Garnier, B. Tinland, H. Ren, C. Desruisseaux, L. C. McCormick, G. Drouin, G. W. Slater *Electrophoresis*. **2001**, 22, 2424-2432.